ELSEVIER

Physics Letters A 303 (2002) 318–327

PHYSICS LETTERS A

www.elsevier.com/locate/pla

Non-Markovian correlation function and direct analysis of spontaneous emission of an excited two-level atom

Chang-qi Cao [a,*], Jin-rong Tian [a], Hui Cao [b]

[a] *Department of Physics, Peking University, Beijing 100871, China*
[b] *Department of Physics and Astronomy, Northwestern University, Evanston, IL 60208-3112, USA*

Received 27 February 2002; received in revised form 14 September 2002; accepted 17 September 2002

Communicated by P.R. Holland

Abstract

The appearance of real correlation function for spontaneous emission is explicitly presented. The non-Markovian correction is calculated directly by the integro-differential equation. The results are compared with the previous results obtained by stochastic quantum trajectory analysis. Obvious difference appears for smaller γ_A/ω_0. The present analysis is believed more reliable.
© 2002 Elsevier Science B.V. All rights reserved.

1. Introduction

It is known for a rather long time [1] that a dynamical system with spectrum bounded below could not have a purely exponential decay. After some early works [2,3], quite a few authors presented the explicit corrections from the Weisskopf–Wigner law for the spontaneous decay of hydrogen or hydrogen-like atoms in the nineteen seventies and eighties [4–8]. All of these calculated deviations are called as non-Markovian corrections, although, strictly speaking, not all of them are due to the non-whiteness of the spectrum, as will be explained in the following.

In Refs. [4–6], the radiating atom is taken as a point-like electric dipole, with the effect of finite size of atom neglected. For this kind of point-like electric dipole, the corresponding correlation spectrum diverges linearly with ω. Hence a cutoff frequency is needed to be introduced, and there exist different conclusions on whether the value of cutoff will affect the decay behavior [6]. The finite-size effect has been considered in Refs. [7,8], which provides a gradually cutdown of the correlation spectrum, and thus exhibits its real appearance.

All of these papers [4–8] applied the Laplace transform to solve the resultant integro-differential dynamical equations. Although the treatment of the Laplace transformed equation becomes quite easy, the mathematical difficulties appear when one carries out the inverse transform. Hence, various kinds of approximation were used. Some papers even made perturbation approximation on the dynamical equation before Laplace transform.

Seke and Herfort made a detailed study on the inverse Laplace transform in their second paper of Ref. [8]. They deformed the path of integration to a

* Corresponding author.
E-mail addresses: cqcao@pku.edu.cn (C.-q. Cao), h-cao@northwestern.edu (H. Cao).

0375-9601/02/$ – see front matter © 2002 Elsevier Science B.V. All rights reserved.
PII: S0375-9601(02)01313-0

special one used by Davidovich and Nussenzveig [9]. In this special path the integrand behaves much better, hence they could give the detailed error estimations. After lengthy and complicated calculation, they obtained the corrections in the whole range, which in the end tail is the same as that of Knight and Milonni [4], and also of that of Robisco [7].

Most of the above cited reference papers, except Refs. [6] and [7], are restricted to the case of $Z = 1$. The obtained deviations for the hydrogen atom are extremely small, only comparable to the Weisskopf–Wigner result in the far remote tail of the decay, when the atom is practically dropped to the lower level.

Carrazana and Vetri [6] also pointed out that the deviation from exponential decay would also appear in the very beginning of the decay. Actually this can be seen directly from the integro-differential equation. They also considered the case of hydrogen-like atom corresponding to large atomic number Z, since large Z will lead to large deviation from Weisskopf–Wigner result. But the parameter they adopted corresponds to unrealistically large value of Z. Moreover, for such large value of Z, the point-like dipole spectrum is certainly inapplicable.

Robisco [7] also considered the case of $Z > 1$. In his treatment, the finite-size effect was taken into account as well. But he did not give the error estimation, and the approximation made in his calculation seems dubious for large Z.

Recently two of us (C.-q. Cao and H. Cao) and other coworkers have restudied this problem by a totally different approach [10]. The generalized quantum trajectory analysis [11,12] is used in that investigation. First, the non-Markovian correlation spectrum is derived generally and also without the point-like electric dipole approximation, then a specific example of allowed transition is taken to make concrete analysis.

The correction to the Weisskopf–Wigner result actually comes from two factors. The first one is the difference between the Einstein A coefficient γ_A, which is taken as the decay rate in Weisskopf–Wigner approach, and the real decay rate γ which takes into account the effect of finite atom size (and the contribution of higher multipole transition, if any). The second factor is the genuine non-Markovian correction originating from the non-uniformity of the real correlation spectrum. The example considered in Ref. [10] is the spontaneous emission of a hydrogen-like atom decaying from state $2P_{1/2}$ to $1S_{1/2}$ as in Refs. [4–8]. The parameter is taken as γ_A/ω_0 which relates to the atomic number Z as

$$\gamma_A/\omega_0 = 4\left(\frac{2}{3}\right)^9 \alpha^3 Z^2, \tag{1}$$

with α denoting the fine structure constant. In the numerical calculation there, the values of γ_A/ω_0 are taken as 10^{-3} and 10^{-4} which is much smaller than 10^{-1} and 10^{-2} taken in Ref. [6], and correspond to $Z = 157$ and $Z = 50$, respectively. In the former case, both corrections specified above are notable, while in the latter case, the first correction due to the difference of γ and γ_A is rather small but still recognizable. The second correction (genuine non-Markovian) remains the same order of that in the former case.

In Ref. [10], the first correction is evaluated analytically and hence reliable, while the evaluation of the second correction by the generalized quantum stochastic trajectory approach suffers two problems. The first one is that the program-generated random number is actually a kind of pseudo random number. When the step interval Δt is decreased, the result not always becomes better, beyond a limit it even becomes worse. The second error comes from the simulation of the real non-Markovian correlation spectrum by a sum of a few Lorentzian spectra. There exists certain disparity between these two spectra, especially in the case of smaller γ_A/ω_0. These problems make the quantity of the second correction not so definite.

The situation mentioned above on Ref. [10] leads us to try another different approach to study the same problem. That is the motive of this Letter.

In this Letter we adopt a straightforward approach, namely solving resultant integro-differential equation by direct numerical calculation. To this end we first evaluate the real correlation function from the corresponding correlation spectrum, and compare it with the approximate correlation function corresponding to the simulated correlation spectrum given in Ref. [10]. To our knowledge, it is the first time the appearance of the real correlation function is explicitly shown. Then the decay of the atomic upper level population is derived numerically. The present result shows the genuine non-Markovian correction becomes considerably smaller than that obtained in Ref. [10] in the case $\gamma_A/\omega_0 = 10^{-4}$, but the total correction to the

Weisskopf–Wigner result is still evident and seems much larger than that of Ref. [7].

Besides, in the approach of this Letter the light field is not taken as reservoir but as a part of the whole dynamical system. So we can studied the properties of emitted light field directly, such as its line profile and degrees of coherence.

2. The correlation function of the spontaneous emission

We take the interaction picture in our approach.

In the rotating wave approximation, the interaction Hamiltonian between a two-level atom and photons is know as

$$\widehat{H}_{\rm int}(t) = i\hbar \sum_{\mathbf{k},j} \big[g_{\mathbf{k}j}\hat{\sigma}_+ \hat{a}_{\mathbf{k}j} e^{i(\omega_0-\omega)t} - g^*_{\mathbf{k}j}\hat{\sigma}_- \hat{a}^\dagger_{\mathbf{k}j} e^{-i(\omega_0-\omega)t} \big], \tag{2}$$

where $\hat{\sigma}_+$ ($\hat{\sigma}_-$) is the atom-level upward (downward) change operator, $\hat{a}_{\mathbf{k}j}$ ($\hat{a}^\dagger_{\mathbf{k}j}$) is the photon annihilation (creation) operator of mode $(\mathbf{k}, j)$ with j denoting the polarization, $g_{\mathbf{k}j}$ is the corresponding coupling constant.

It is easy to see that under the above interaction the state vector of our system can be expressed as

$$|t\rangle = C_2(t)|\phi_2; 0\rangle + \sum_{\mathbf{k},j} C_{1,\mathbf{k}j}(t)|\phi_1; \mathbf{k}, j\rangle, \tag{3}$$

where $|\phi_2; 0\rangle$ denotes the state with atom in the upper level (level 2) and no photon exists therein, $|\phi_1; \mathbf{k}, j\rangle$ denotes the state with the atom in the lower level (level 1) and with one photon in the mode $(\mathbf{k}, j)$. The initial condition is taken as

$$C_2(0) = 1, \qquad C_{1,\mathbf{k}j}(0) = 0. \tag{4}$$

The coefficients $C_2(t)$ and $C_{1,\mathbf{k}j}(t)$ satisfy the following dynamical equations

$$\frac{d}{dt}C_{1,\mathbf{k}j}(t) = -g^*_{\mathbf{k}j} e^{i(\omega-\omega_0)t} C_2(t), \tag{5a}$$

$$\frac{d}{dt}C_2(t) = \sum_{\mathbf{k}j} g_{\mathbf{k}j} e^{-i(\omega-\omega_0)t} C_{1,\mathbf{k}j}(t). \tag{5b}$$

From Eqs. (5), one readily gets the following integro-differential equation for $C_2(t)$

$$\frac{d}{dt}C_2(t) = -\int_0^t U(t-t')C_2(t')\,dt', \tag{6}$$

in which

$$U(t-t') = \sum_{\mathbf{k}j} |g_{\mathbf{k}j}|^2 e^{-i(\omega-\omega_0)(t-t')} \equiv \int_0^\infty R(\omega) e^{-i(\omega-\omega_0)(t-t')}\,d\omega \tag{7}$$

for $0 \leqslant t' \leqslant t$. The $R(\omega)$, which is the real correlation spectrum, is given by

$$R(\omega) = \frac{e^2\hbar\omega}{4\pi^2 m^2 c^3} \int d\Omega_k \big[|\mathbf{G}_\mathbf{k}|^2 - |\mathbf{n}_\mathbf{k}\cdot\mathbf{G}_\mathbf{k}|^2 \big] \tag{8}$$

with

$$\mathbf{G}_\mathbf{k} = \int e^{i\mathbf{k}\cdot\mathbf{x}} \psi_2^\dagger(\mathbf{x}) \nabla \psi_1(\mathbf{x})\, d^3x. \tag{9}$$

The $U(t-t')$ given above is the correlation function for the spontaneous emission of the atom, which describes the dependence of the variation rate of $C_2(t)$ on its past value $C_2(t')$ $(t' < t)$.

To see explicitly the correlation function $U(\tau)$, we consider the same example studied in Refs. [7,8,10], namely the hydrogen-like atom with two levels $1S_{1/2}$ and $2P_{1/2}$. The corresponding correlation spectrum, calculated in Ref. [10] by the Schrödinger wave functions of the two levels, is given by

$$R(\omega) = \frac{\gamma_A}{2\pi\omega_0} \frac{\omega}{(1+\frac{a^2\omega^2}{c^2})^4}, \tag{10}$$

in which the factor $\frac{\gamma_A}{2\pi\omega_0}\omega$ is the universal point electric-dipole correlation spectrum, and $(1+\frac{a^2\omega^2}{c^2})^4$ is the cut down factor due to the finite size of the atom, which is the same as those used in Refs. [7,8].

The only free parameter in this example is Z, the atomic number. All the parameters in Eq. (10) are related to Z by

$$a = \frac{2}{3}\frac{\hbar^2}{me^2}\frac{1}{Z}, \tag{11a}$$

$$\omega_0 = \frac{3}{8}\alpha^2 \frac{mc^2}{\hbar} Z^2, \tag{11b}$$

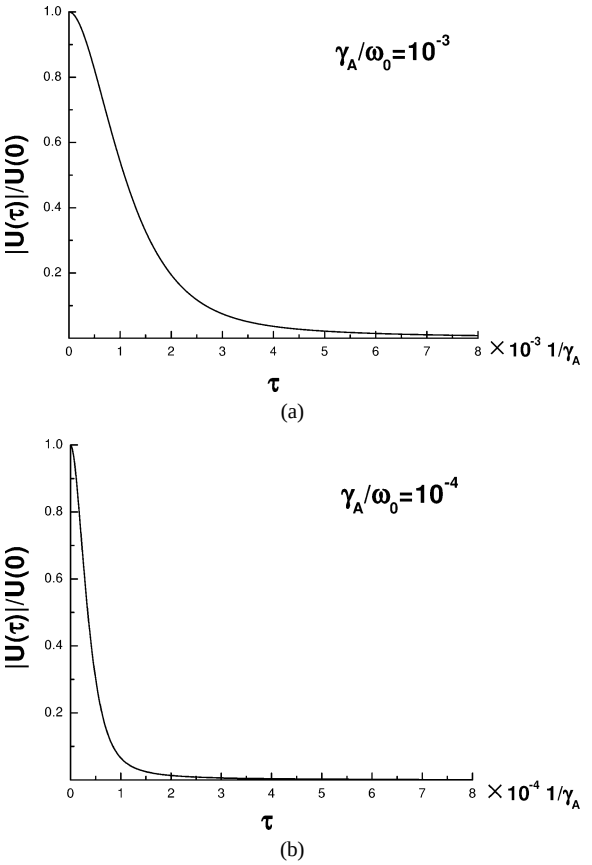

Fig. 1. The absolute value of $U(\tau)$ as function of τ. τ is in unit of $1/\gamma_A$. (a) The parameter $\gamma_A/\omega_0 = 10^{-3}$, (b) $\gamma_A/\omega_0 = 10^{-4}$.

$$\gamma_A = \left(\frac{4}{9}\right)^4 \alpha^5 \frac{mc^2}{\hbar} Z^4, \tag{11c}$$

with α denoting the fine structure constant. The correlation function $U(\tau)$ for this example is given hence by

$$U(\tau) = F(\tau)e^{i\omega_0\tau}, \quad 0 \leqslant \tau \leqslant t, \tag{12a}$$

in which $F(\tau)$ is conventional Fourier transform of $R(\omega)$:

$$F(\tau) = \int_0^\infty R(\omega)e^{-i\omega\tau}\,d\omega = \frac{\gamma_A}{2\pi\omega_0}\int_0^\infty \frac{\omega}{(1+a^2\omega^2/c^2)^4}e^{-i\omega\tau}\,d\omega. \tag{12b}$$

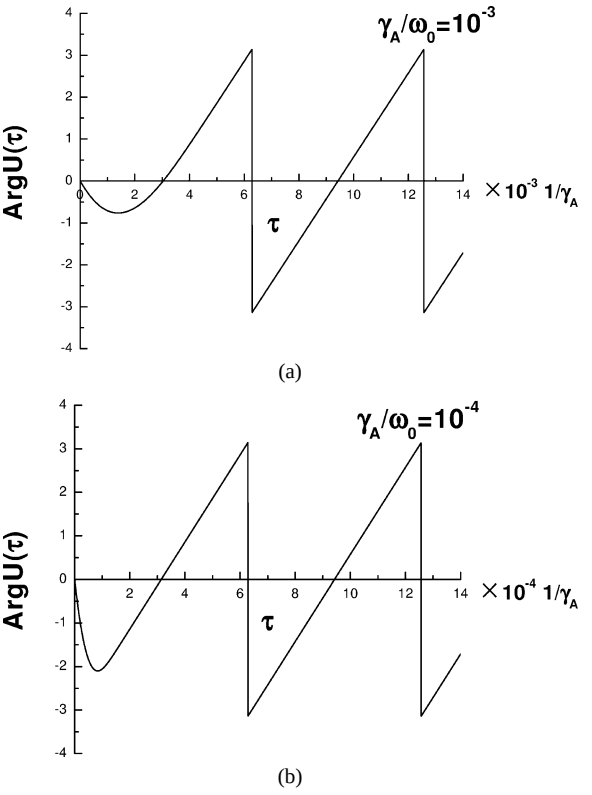

Fig. 2. The argument of $U(\tau)$ as function of τ (in unit of $1/\gamma_A$). (a) The parameter $\gamma_A/\omega_0 = 10^{-3}$, (b) $\gamma_A/\omega_0 = 10^{-4}$.

The imaginary part of $F(\tau)$ can be easily calculated by contour integration, since its integrand is an even function of ω. But the real part of that integral cannot be evaluated in the same way. So we have to use the numerical calculation to evaluate $U(\tau)$. The results are shown in Figs. 1 and 2. The free parameter is taken as γ_A/ω_0 instead of Z, the relation between these two dimensionless parameters is

$$\gamma_A/\omega_0 = \frac{1}{6}\left(\frac{64}{81}\right)^2 \alpha^3 Z^2. \tag{13}$$

For comparison with Ref. [10], we still take $\gamma_A/\omega_0 = 10^{-3}$ and 10^{-4}. The value $\gamma_A/\omega_0 = 10^{-3}$ used in Figs. 1(a) and 2(a) corresponds to $Z = 157$, somewhat larger than the upper limit of the real nuclei. The value $\gamma_A/\omega_0 = 10^{-4}$ for Figs. 1(b) and 2(b) corresponds to $Z = 50$.

Fig. 1 shows $|U(\tau)|/U(0)$ vs. τ, while Fig. 2 shows Arg $U(\tau)$ vs. τ. The unit of τ in the abscissa is taken as $1/\gamma_A$, since it still characterizes the time scale of

decay even in the non-Markovian approach. The value of $U(0)$ may be analytically derived with the result

$$\frac{U(0)}{\gamma_A^2} = \frac{1}{12\pi\omega_0\gamma_A}\left(\frac{c}{a}\right)^2 = \frac{2}{9\pi}\left(\frac{64}{81}\right)^2\alpha\left(\frac{\omega_0}{\gamma_A}\right)^2. \quad (14)$$

We see from Fig. 1 that the peak of $\frac{|U(\tau)|}{U(0)}$ has a width of order $1/\omega_0$, the proportional coefficient decreases when γ_A/ω_0 decreases. Fig. 2 shows outside the peak $\arg U(\tau)$ quickly approaches its asymptotic value $\omega_0\tau - \pi$.

The correlation function corresponding to point electric-dipole spectrum can be derived analytically:

$$U_D(\tau) = \frac{\gamma_A}{2\pi\omega_0}\int_0^\infty \omega e^{-i(\omega-\omega_0)\tau}\,d\omega = \frac{\gamma_A}{2\pi\omega_0}\lim_{\varepsilon\to 0}\int_0^\infty \omega e^{-i(\omega-\omega_0)\tau-\varepsilon\tau}\,d\omega = \frac{\gamma_A}{2\pi\omega_0}\frac{1}{\tau^2}e^{i\omega_0\tau}. \quad (15)$$

It diverges as $\tau \to 0$, and hence is meaningless.

If one approximate the cut-down factor

$$\left(1+\frac{a^2\omega^2}{c^2}\right)^{-4}$$

by $e^{-\beta\omega}$, the corresponding correlation function is given by

$$U_A(\tau) = \frac{\gamma_A}{2\pi\omega_0}\frac{1}{\tau^2+\beta^2}e^{i\omega_0\tau+2i\theta_\tau}, \quad 0 \leqslant \tau \leqslant t, \quad (16)$$

$\theta_\tau = \tan^{-1}(-\frac{\tau}{\beta})$, hence θ_τ changes quickly from zero to $-\pi/2$ as τ increases, in case β is a small time interval.

As mentioned above the phase factor of the correlation function $U(\tau)$ soon approaches its asymptotic value $\exp[i(\omega_0\tau - \pi)]$, like $U_A(\tau)$ for small β. The calculated value of $|U(\tau)|$ is also similar to

$$\frac{U(0)}{\tau^2+\beta^2}$$

($\beta \cong 1/\omega_0$ for $\gamma_A/\omega_0 = 10^{-3}$ as shown in Fig. 3).

We now compare the real correlation function $U(\tau)$ with its Markovian approximation $-(\gamma + 2i\delta\omega_0)\delta(\tau)$.

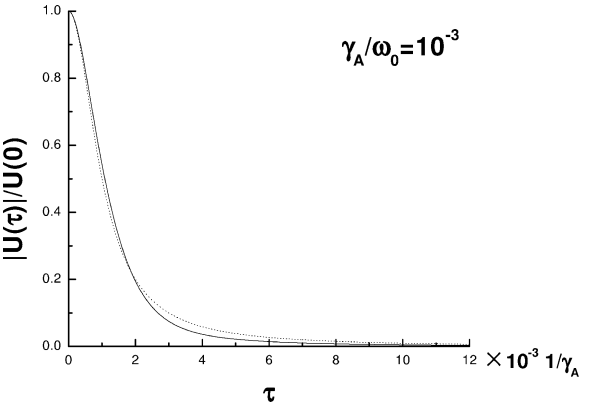

Fig. 3. The simulation of $|U(\tau)|/U(0)$ by $1/(\omega_0^2\tau^2+1)$. Solid line represents $|U(\tau)|/U(0)$; dotted line represents $1/(\omega_0^2\tau^2+1)$.

It is known that $\delta(\tau)$ can be expressed by different limit form, such as

$$\delta(\tau) = \frac{1}{\pi}\lim_{\varepsilon\to 0}\frac{\varepsilon}{\tau^2+\varepsilon^2} \quad (17a)$$

and

$$\delta(\tau) = \frac{1}{\pi}\lim_{\omega\to\infty}\frac{\sin\omega\tau}{\tau}. \quad (17b)$$

The first form (17a) is always of positive value and has typical peaked form with infinitesimal width 2ε. So it tends to zero for $\tau > 0$. The value of form (17b) alternates with time and its absolute value decays rather slowly as $\sim 1/\tau$. However, the infinite oscillation frequency makes its value effectively drop to zero for $\tau > 0$ too.

We have shown that the real correlation function $U(\tau)$ has both the peaked form and oscillating behavior outside the peak region. The oscillation frequency is ω_0 and the peak width is of order $1/\omega_0$. These two factors together make $U(\tau)$ approximate δ-function when it is applied to functions with variation rate much smaller than ω_0. Since the variation rate of spontaneous emission is of order γ_A, the condition for validity of Markovian approximation is therefore given by

$$\frac{\gamma_A}{\omega_0} \ll 1. \quad (18)$$

Next let us investigate the approximate correlation function $U_s(\tau)$ corresponding to the simulation corre-

lation spectrum [10] $R_s(\omega)$ for $\gamma_A/\omega_0 = 10^{-3}$:

$$R_s(\omega) = \frac{\omega_0}{2\pi}\left[\frac{|g_1|^2\Gamma_1}{(\omega-\omega_1)^2+\frac{1}{4}\Gamma_1^2} + \frac{|g_2|^2\Gamma_2}{(\omega-\omega_2)^2+\frac{1}{4}\Gamma_2^2}\right],$$

with

$$\omega_1/\omega_0 = 1, \qquad g_1/\omega_0 = 0.011, \qquad \Gamma_1/\omega_0 = 1.3,$$
$$\omega_2/\omega_0 = 1.85, \qquad g_2/\omega_0 = 0.018, \qquad \Gamma_2/\omega_0 = 2.4.$$

The integration range of ω is now extended to $(-\infty, +\infty)$, hence $U_s(\tau)$ has the following analytical expression:

$$U_s(\tau) = \omega_0\left[\frac{1}{\Gamma_1}|g_1|^2 e^{-i(\omega_1-\omega_0)\tau-\frac{1}{2}\Gamma_1\tau} + \frac{1}{\Gamma_2}|g_2|^2 e^{-i(\omega_2-\omega_0)\tau-\frac{1}{2}\Gamma_2\tau}\right] \cong \omega_0^2\times 10^{-4}\left[0.93e^{-0.65\omega_0\tau} + 1.35e^{-i0.85\omega_0\tau-1.2\omega_0\tau}\right]. \quad (19)$$

When τ becomes larger, the first term soon becomes dominant, so $U_s(\tau)$ drops down exponentially with a comparatively large rate $\Gamma_1/2$ of order ω_0, but without oscillation. We see that $U_s(\tau)$ has a quite different behavior from $U(\tau)$.

3. Non-Markovian correction to the atom decay

In Ref. [10], the non-Markovian effect on the decay of the atom upper-level population is investigated by the quantum trajectory analysis of an enlarged system. For the example studied there, the transition is pure electric dipole transition, so the correction is solely due to the finite size of the atom and non-uniformity of correlation spectrum. As mentioned in Section 1, the correction to Weisskopf–Wigner result [13] results from two factors. The first factor comes from the use of real decay rate γ instead of γ_A, but the finiteness of correlation time is still ignored (cf. Eq. (25)). This factor is evaluated analytically and hence is reliable. The second factor is due to finiteness of correlation time. Its evaluation in Ref. [10] is quantitatively not so accurate. In this Letter we will solve the integro-differential equation (6) numerically step by step with the initial condition $C_2(0) = 1$. If we denote $n\Delta t$ by t_n, the recurrence formula may be simply taken as

$$C_2(t_{n+1}) \cong C_2(t_n) - \sum_{m=1}^{n}(\Delta t)^2 U(t_m)C_2(t_{n-m}), \quad (20)$$

other more skilled method may also be applied.

Fig. 4(a) and (b) show the so obtained evolutions of the upper level population $N_2(t) = |C_2(t)|^2$ and compare them with the results with Markov approximation based on the real correlation spectrum (namely to use the real decay rate γ instead of γ_A) and also with the Weisskopf–Wigner results. The latter two curves are identical to those in Ref. [10]. We see that in the

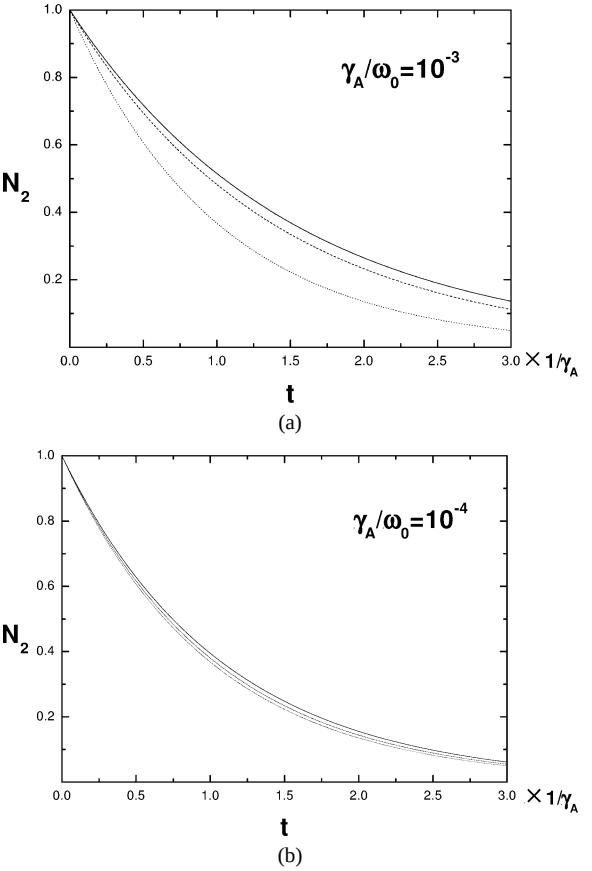

Fig. 4. The evolution of atom upper-level population $N_2(t)$. Solid line is the numerically calculated result without Markov approximation; dash line is the result with Markov approximation on the real correlation spectrum; dotted line represents Weisskopf–Wigner result. (a) The parameter γ_A/ω_0 is taken as 10^{-3}. (b) The parameter γ_A/ω_0 is taken as 10^{-4}.

Table 1
The five sets of parameter of imitation

A	γ'
$-0.018\gamma_A$	$0.627\gamma_A$
$-0.014\gamma_A$	$0.635\gamma_A$
0	$0.663\gamma_A$
$0.01\gamma_A$	$0.683\gamma_A$
$0.036\gamma_A$	$0.735\gamma_A$

case $\gamma_A/\omega_0 = 10^{-3}$ the correction due to this second factor (i.e., the difference between the upper curve and the middle curve) is of the same sign as that in Ref. [10], but quantitatively somewhat smaller. In the case $\gamma_A/\omega_0 = 10^{-4}$, this second correction is much smaller than that presented in Ref. [10]. However, the total difference from the Weisskopf–Wigner result is still evident.

Next, we inspect whether the exact (numerically calculated) result $N_2(t)$ (solid line) in Fig. 4(a) (corresponding $\gamma_A/\omega_0 = 10^{-3}$) still may be approximated by an exponential decay in the range of $\gamma_A t$ from nearly zero to three. If we simulate $C_2(t)$ by

$$(1 + At)e^{-\frac{\gamma'}{2}t - i\delta\omega' t},$$

namely simulate $N_2(t)$ by

$$(1 + At)^2 e^{-\gamma' t}$$

with the factor $(1 + At)^2$ representing the deviation from an exponential decay, the results of numerical fitting show that the five sets of parameters in Table 1 all generate practically identical curves with the exactly calculated curve (the solid line in Fig. 4(a)) as shown in Fig. 5.

The above results mean that $N_2(t)$ practically still has an exponential behavior in this finite range (the very beginning stage which deviates exponential decay as shown in Fig. 3 of Ref. [10] is too small to be recognized in Fig. 4(a)), but with an effective decay constant

$$\gamma_{\text{eff}} = 0.663\gamma_A, \tag{21}$$

which is smaller than the real decay rate

$$\gamma = 2\pi R(\omega_0) = 0.729\gamma_A.$$

This behavior of exponential decay does not mean that $U(t - t')$ is still proportional to $\delta(t - t')$, because

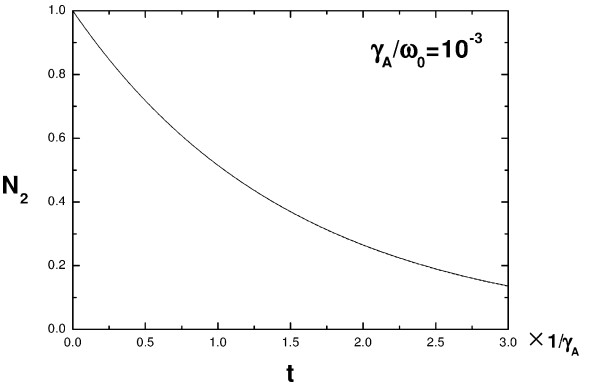

Fig. 5. The simulation of exact (numerically calculated) result without Markov approximation. All the five simulating curves with parameters specified in Table 1 coincide with the exact result, the solid line in Fig. 4(a).

this behavior is limited in finite interval. Let us do a little more inspect on this point.

Under this zero correlation-time supposition, Eq. (6) reduces to

$$\frac{d}{dt}C_2(t) = -C_2(t)\int_0^t U(t - t')\,dt'. \tag{22}$$

Let

$$\frac{1}{2}\Gamma(t) \equiv \int_0^t U(t - t')\,dt', \tag{23}$$

substitute Eq. (7) into the right-hand side of Eq. (23) and carry out the integration over t', one gets

$$\operatorname{Re}\Gamma(t) = 2\int_0^\infty R(\omega)\frac{\sin(\omega - \omega_0)t}{\omega - \omega_0}\,d\omega. \tag{24}$$

In case the above supposition agrees with our numerical investigation, the right side of Eq. (24) should equal to γ_{eff} given by Eq. (21) except for the very beginning of t.

To check this, we take five values of t in Eq. (24): $(0.1, 0.5, 1, 2, 3)\frac{1}{\gamma_A}$, all the $\operatorname{Re}\Gamma(t)$ numerically calculated according to Eq. (24) are still $0.729\gamma_A$ up to three significant figures, which is just γ not γ_{eff}. Hence the supposition that $U(t - t')$ is proportional to $\delta(t - t')$ for $\gamma_A/\omega_0 = 10^{-3}$ is not true, the difference between the upper curve and middle curve is a genuine non-Markov correction.

We may also see this by analytical inspection. For t larger than the effective correlation time τ_c, which is of order $1/\omega_0$, the integration limit $(0,t)$ in Eq. (23) may be extended to $(-\infty,t)$, then

$$\begin{aligned}\frac{1}{2}\Gamma(t) &= \int_{-\infty}^{t} U(t-t')\,dt' \\ &= \lim_{\varepsilon\to 0}\int_{-\infty}^{t} dt' \int_{0}^{t} d\omega\, R(\omega) e^{-i(\omega-\omega_0-i\varepsilon)(t-t')} \\ &= \lim_{\varepsilon\to 0}\int_{0}^{\infty} R(\omega)\frac{-i}{\omega-\omega_0-i\varepsilon}\,d\omega \\ &= \int_{0}^{\infty} R(\omega)\left[\pi\delta(\omega-\omega_0) - i\wp\frac{1}{\omega-\omega_0}\right]d\omega,\end{aligned} \tag{25a}$$

leading to usual result

$$\operatorname{Re}\Gamma(t) = 2\pi R(\omega_0) = \gamma, \tag{25b}$$

which has the value of $0.729\gamma_A$, not γ_{eff} given by Eq. (21).

4. The line profile and degrees of coherence of emitted light

As mentioned in Section 1, in our approach the light field is not eliminated from the dynamical system as a reservoir, so we may inspect the features of the emitted photon directly from the value of $C_{1,\mathbf{k}j}(t)$, which may be obtained by substituting $C_2(t)$ into Eq. (5a) and integrating over t.

Since $C_2(t)$ is well approximated by

$$C_2(t) = e^{-\frac{1}{2}\gamma_{\text{eff}}t - i\delta\omega_0 t}$$

even for Z as large as 157 (corresponding to $\gamma_A/\omega_0 = 10^{-3}$), the result of $C_{1,\mathbf{k}j}(t)$ is easily evaluated and given by

$$C_{1,\mathbf{k}j}(t) = \frac{ig^*_{\mathbf{k}j}}{(\omega-\omega_0)+\frac{1}{2}i\gamma_{\text{eff}}}\left[e^{i(\omega-\omega_0)t-\frac{1}{2}\gamma_{\text{eff}}t}-1\right], \tag{26}$$

with $\delta\omega_0$ already incorporated in ω_0.

When $t\to\infty$, the atom completely jumps to the lower state with one photon emitted. The probability of the emitted photon in mode $(\mathbf{k}, j)$ is $|C_{1,\mathbf{k}j}(\infty)|^2$. To derive the line profile, we first transfer the summation over $\mathbf{k}$ to integration, then carry out the integration over the direction angle of $\mathbf{k}$. After further summation over j, we readily get the photon distribution over ω as

$$\begin{aligned}P(\omega) &= \sum_j \int \frac{\omega^2\,d\Omega_k}{c^3}\frac{V}{(2\pi)^3}\left|C_{1,\mathbf{k}j}(\infty)\right|^2 \\ &= \frac{R(\omega)}{(\omega-\omega_0)^2+\frac{1}{4}\gamma_{\text{eff}}^2}.\end{aligned} \tag{27}$$

Eq. (27) indicates the photon frequency distribution is a product of the correlation spectrum and a Lorentzian factor with linewidth γ_{eff}. Since $R(\omega)$ varies little over the range of a few γ_{eff} around ω_0, the line profile is practically Lorentzian. The non-Markovian effect just lies in the change of linewidth to γ_{eff}.

One may also define photon "frequency" distribution for any $t>0$ as

$$\begin{aligned}P(\omega,t) &= \sum_j \int \frac{\omega^2\,d\Omega_k}{c^3}\frac{V}{(2\pi)^3}\left|C_{1,\mathbf{k}j}(t)\right|^2 \\ &= \frac{R(\omega)}{(\omega-\omega_0)^2+\frac{1}{4}\gamma_{\text{eff}}^2} \\ &\quad\times\left[1-2e^{-\frac{1}{2}\gamma_{\text{eff}}t}\cos(\omega-\omega_0)t+e^{-\gamma_{\text{eff}}t}\right].\end{aligned}$$

Actually $P(\omega,t)$ is the distribution among wave number according to the relation $\omega = kc$. We see from $P(\omega,t)$ that the photon's "frequency" is always limited within a narrow range of width γ_{eff} around ω_0, but with a time-varying coefficient. For $\omega=\omega_0$, this coefficient increases with t monotonically from zero to approach 1, for $\omega\neq\omega_0$, it approaches 1 by damped oscillation, so the profile varies with time.

Next let us turn to the coherence functions of the emitted field. The coherence functions are originally defined in Heisenberg picture, they should be first transfered to the interaction picture. Note that the state vector $|\rangle$ and operators $\hat{L}$ in these two pictures are connected by

$$|\rangle^H = \widehat{U}(0,t)|t\rangle, \qquad \hat{L}^H(t) = \widehat{U}(0,t)\hat{L}(t)\widehat{U}(t,0) \tag{28}$$

in which $\widehat{U}(t,t')$ is the evolution operator in interaction representation from t' to t, $|t\rangle$ and $\hat{L}(t)$ are also state vector and operator in interaction picture, with the upper index I omitted.

The first and second order of coherence functions in interaction picture are readily obtained by utilizing Eq. (28) with the results

$$G^{(1)}(\mathbf{x}, t_2; \mathbf{x}, t_1) = \sum_l \langle t_2 | \widehat{E}_l^{(-)}(\mathbf{x}, t_2) \widehat{U}(t_2, t_1) \widehat{E}_l^{(+)}(\mathbf{x}, t_1) | t_1 \rangle,$$

$$G^{(2)}(\mathbf{x}, t_2; \mathbf{x}, t_1) = \sum_{l,l'} \langle t_1 | \widehat{E}_l^{(-)}(\mathbf{x}, t_1) \widehat{U}(t_1, t_2) \widehat{E}_{l'}^{(-)}(\mathbf{x}, t_2) \times \widehat{E}_{l'}^{(+)}(\mathbf{x}, t_2) \widehat{U}(t_2, t_1) \widehat{E}_l^{(+)}(\mathbf{x}, t_1) | t_1 \rangle. \quad (29)$$

Since

$$\begin{aligned} \widehat{\mathbf{E}}^{(+)}(\mathbf{x}, t) | t_1 \rangle &= \sum_{\mathbf{k}, j} \sqrt{\frac{2\pi\hbar\omega}{V}}\, \mathbf{e}_{\mathbf{k}j} \hat{a}_{\mathbf{k}j} e^{i\mathbf{k}\cdot\mathbf{x} - i\omega t_1} | t_1 \rangle \\ &= \sum_{\mathbf{k}, j} \sqrt{\frac{2\pi\hbar\omega}{V}}\, \mathbf{e}_{\mathbf{k}j} C_{1,\mathbf{k}j}(t_1) e^{i\mathbf{k}\cdot\mathbf{x} - i\omega t_1} | \phi_1, 0 \rangle \\ &= \mathcal{E}(\mathbf{x}, t_1) | \phi_1, 0 \rangle \end{aligned} \quad (30)$$

and

$$\widehat{U}(t_2, t_1) | \phi_1, 0 \rangle = | \phi_1, 0 \rangle \quad (31)$$

under rotating-wave approximation, we get

$$G^{(1)}(\mathbf{x}, t_2; \mathbf{x}, t_1) = \mathcal{E}^*(\mathbf{x}, t_2) \cdot \mathcal{E}(\mathbf{x}, t_1). \quad (32)$$

Actually from the conservation of angular momentum and parity, the emitted photon field in our example should have angular momentum $J = 1$ and negative parity, hence it is just the electric dipole field. In the wave zone, $\mathcal{E}(\mathbf{x}, t)$ has the form of spherical wave function with polarization vector ξ perpendicular to $\mathbf{x}$. Write $\mathcal{E}(\mathbf{x}, t)$ as $\varepsilon(\mathbf{x}, t)\xi$, we get accordingly

$$G^{(1)}(\mathbf{x}, t_2; \mathbf{x}, t_1) = \varepsilon^*(\mathbf{x}, t_2)\varepsilon(\mathbf{x}, t_1). \quad (33)$$

Although $G^{(1)}(\mathbf{x}, t_2; \mathbf{x}, t_1)$ varies with time, the first order degree of coherence $g^{(1)}(\mathbf{x}, t_2; \mathbf{x}, t_1)$, which is given by

$$\frac{G^{(1)}(\mathbf{x}, t_2; \mathbf{x}, t_1)}{|\varepsilon(\mathbf{x}, t_2)||\varepsilon(\mathbf{x}, t_1)|},$$

has its absolute value identical to one in the wave zone, for any positive t_1 and t_2.

Utilizing Eqs. (30) and (31), it is easy to see that $G^{(2)}(\mathbf{x}, t_2; \mathbf{x}, t_1)$ is identically zero as expected, since $|t\rangle$ at most contains one photon.

5. Summary

(1) The correlation function of spontaneous emission is investigated in some detail. Although we use an example to get concrete results, the following features may have general meaning.

The correlation function $U(\tau)$ commonly has the expression

$$U(\tau) = f(\tau) e^{i\omega_0\tau}$$

in which

$$f(\tau) = \int_0^\infty R(\omega) e^{-i\omega\tau}\, d\omega,$$

with $R(\omega)$ being zero at $\omega = 0$, and dropping down for large ω. The absolute value $|f(\tau)|$ decreases as τ increases because the factor $e^{-i\omega\tau}$ oscillates more quickly with ω for larger τ. This leads to a peak shape of $|f(\tau)|$. The peak width in our example is of order $1/\omega_0$. The $U(\tau)$ approximate δ-function not only due to the drop of $|f(\tau)|$, but also due to the rapid oscillating factor $e^{i\omega_0\tau}$. The oscillating frequency ω_0 is large as compared with the decay rate. However it is a finite value, while a genuine δ-function has limiting forms

$$\delta(\tau) = \lim_{\omega\to\infty} \frac{\sin\omega\tau}{\pi\tau} \quad \text{or} \quad \frac{1}{\pi} \lim_{\varepsilon\to 0} \frac{\varepsilon}{\tau^2 + \varepsilon^2},$$

the former has an oscillating frequency ω that tends to infinity, and the latter has an infinitesimal width ε. This difference between $U(\tau)$ and $\delta(\tau)$ causes non-Markovian corrections when γ_A/ω_0 becomes not very small.

(2) The Weisskopf–Wigner result is good for hydrogen-like atom only for relatively small Z. For $Z = 50$, the difference between the non-Markovian result and the Weisskopf–Wigner result is already obvious.

The upper-level population practically still shows exponential decay in the period for $t = 0$ up to $3/\gamma_A$, even when the non-Markovian correction is relatively large as in the case $\gamma_A/\omega_0 = 10^{-3}$.

(3) The line profile is shown in general to be the product of correlation spectrum and a usual Lorentzian factor with width γ_{eff}. However practically it shows no deviation from the Lorentz profile, the non-Markovian effect just lies in the change of linewidth to γ_{eff}.

The coherence functions may be calculated from the state of the emitted field. The absolute value

of first order degree of coherence remains unity for any positive t_1 and t_2. The second order coherence function is identical zero under the rotating-wave approximation.

Acknowledgements

This work is supported by National Natural Science Foundation of China (project number 19774004), and by the International Program of National Science Foundation of USA (ECS-9800068).

References

[1] R. Paley, N. Wiener, Fourier Transforms in the Complex Domain, Providence, RI, 1934.
[2] L.A. Khalfin, Sov. Phys.—Dokl. 1 (1956) 671;
L.A. Khalfin, Sov. Phys.—Dokl. 2 (1957) 340;
L.A. Khalfin, Sov. Phys.—JETP 6 (1958) 1053.
[3] L. Fonda, G.C. Ghirardi, Nuovo Cimento A 7 (1971) 180.
[4] P.L. Knight, P.W. Milonni, Phys. Lett. A 56 (1976) 275.
[5] K. Wodkiewicz, J.H. Eberly, Ann. Phys. 101 (1976) 574.
[6] P. Carrazana, G. Vetri, Nuovo Cimento B 55 (1980) 191.
[7] R.T. Robisco, Phys. Lett. A 100 (1984) 407.
[8] J. Seke, W. Herfort, Phys. Rev. A 38 (1988) 833;
J. Seke, W. Herfort, Phys. Rev. A 40 (1989) 1926.
[9] L. Davidovich, H.M. Nussenzveig, in: A.O. Barut (Ed.), Foundations of Radiation Theory and Quantum Electrodynamics, Plenum, New York, 1980.
[10] Chang-qi Cao, Jikun Wei, Wei Long, Hui Cao, Phys. Rev. A 64 (2001) 43810.
[11] A. Imamoglu, Phys. Rev. A 50 (1994) 3650.
[12] P. Stenius, A. Imamoglu, Quan. Semiclass. Opt. 8 (1996) 283.
[13] V. Weisskopf, E. Wigner, Z. Phys. A 63 (1930) 54.